



Carbohydrate analysis on hybrid poly(dimethylsiloxane)/glass chips dynamically coated with ionic complementary peptide



Nan Li^{a,1}, Xiaoman Hai^{a,1}, Xiaoling Yu^a, Fuquan Dang^{a,b,*}

^a School of Chemistry and Chemical Engineering, Shaanxi Normal University, Xi'an 710119, China

^b Key Laboratory of Analytical Chemistry for Life Science of Shaanxi Province, Xi'an 710119, China

ARTICLE INFO

Article history:

Received 31 August 2016

Received in revised form

15 December 2016

Accepted 16 December 2016

Available online 19 December 2016

Keywords:

Ionic complementary peptide

Dynamic coatings

Hybrid poly(dimethylsiloxane)/glass microchannel

Maltodextrin ladder

Glycan extracts

ABSTRACT

A facile and efficient dynamic coating method using an ionic complementary peptide was established for high-performance separation of 8-aminopyrene-1,3,6-trisulfonic acid (APTS)-labeled carbohydrates in a hybrid poly(dimethylsiloxane) (PDMS)/glass microfluidic channel. EAK16-II with a sequence of [(Ala-Glu-Ala-Glu-Ala-Lys-Ala-Lys)₂] can readily self-organize into a complete coating layer tightly adsorbed on both hydrophobic PDMS and hydrophilic glass surfaces, which efficiently suppressed nonspecific analyte adsorption and minimized electroosmotic flow (EOF). Separation conditions were systematically investigated with respect to EAK16-II concentration, running buffer, buffer pH, and field strength (E_{sep}). Under the optimal conditions, rapid and reproducible separations of maltodextrin ladder, glycans from glucosamine capsules, tablets, and pomegranate peel extracts were achieved with over 450000 theoretical plates per meter in the hybrid PDMS/glass microchannels dynamically coated with 1.0 mg/mL EAK16-II-0.05% *n*-dodecyl β -D-maltoside (DDM), and the relative standard deviation (RSD) values were less than 3.2% ($n=4$) for the migration times. The present work provides a facile and efficient means to minimize EOF and nonspecific analyte adsorption in microfluidic chips fabricated in various substrates, thereby broadening the applications of microfluidic chips in complicated biological assays.

© 2016 Elsevier B.V. All rights reserved.

1. Introduction

Carbohydrates, one of the four major classes of biomass along with proteins, nucleic acids, and lipids, are the most abundant organic matter and biological molecules on Earth since they exist in all living creatures including animals, plants, and bacteria [1–3]. Not only do carbohydrates serve as the main energy stores and fuels, as well as the structural elements in cell walls, of animals and plants, they also play vital roles in mediating cell–cell recognition and the interactions of cells with the cellular environment, making carbohydrate analyses necessary and significant for researchers. However, separation of carbohydrates still remains a challenge owing to the immense structural diversity and heterogeneity of carbohydrates from various natural sources, such as exceptionally high numbers of chiral centers, the wide variety of glycosidic bonds, and the number and position of branched chains [4,5]. Recently, various techniques have been used in the analysis of complex car-

bohydrates, such as mass spectrometry (MS) [6], high performance liquid chromatography (HPLC) [7–11], capillary electrophoresis (CE) [12,13], fluorescence-assisted carbohydrate electrophoresis (FACE) [14], microchip electrophoresis (μ -CE) [15,16], and electrochemical detection (ED) [17], or their combinations [18–22], in plant analysis, fermentation and metabolism studies, pharmaceutical engineering, and food industries. Among these methods, μ -CE is a promising candidate in carbohydrate analysis owing to its unique characteristics of high speed, high throughput, low sample consumption, great integration, miniaturization, and automation [4,15–17].

In recent years, poly(dimethylsiloxane) (PDMS) has become one of the most extensively used materials in laboratories for the fabrication of microfluidic chips [23–29]. The common process for fabricating microfluidic chip is the bonding of a PDMS replica onto a glass slide, forming a hybrid PDMS/glass microfluidic chip with enclosed microchannels [27,30–35]. In biological applications, the use of both highly hydrophobic PDMS and hydrophilic glass generally leads to severe nonspecific analyte adsorption [27–29] and unstable electroosmotic flow (EOF) [30–33], resulting in a decrease in chip performance. To address this intractable problem, a significant amount of work has been directed toward developing methods, mainly including physically adsorbed [15,23,33,36]

* Corresponding author at: School of Chemistry and Chemical Engineering, Shaanxi Normal University, Xi'an 710119, China.

E-mail address: dangfq@snnu.edu.cn (F. Dang).

¹ These authors contributed equally to this work.

and covalent modification [31,32,37], for better use of microfluidic chips. However, the completely different surface properties of PDMS and glass make chip surface modification a huge challenge [27,28]. Generally, covalent modification are case-dependent and multistep processes and are not always suitable for microfluidic chips fabricated in different materials. Dynamic coatings are general and the most widely used surface modification approaches in electrophoretic analysis, in which coating additives, such as water-soluble polymers, surfactants, and amphiphilic molecules dissolved in running buffers, are physically adsorbed on the channel walls to form a coating film for the suppression of EOF and non-specific analyte adsorption [4,15,23,33,36]. Among the additives, polymer additives such as polyethylene glycol (PEG) and methyl cellulose (MC) clearly reduce nonspecific adsorption of analytes and improve separation. However, the addition of concentrated additives in running buffers can easily increase the buffer viscosity or conductivity, leading to rather difficult handling of microfluidic chips. In recent study, we found that ionic complementary peptides EAR16-II [(Ala-Glu-Ala-Glu-Ala-Arg-Ala-Arg)₂] and EAK16-II [(Ala-Glu-Ala-Glu-Ala-Lys-Ala-Lys)₂], with alternating hydrophilic and hydrophobic amino acid residues, show high surface affinity for solid surfaces with negative charges such as PDMS [33] and poly(methyl methacrylate) (PMMA) [36] via ionic hydrogen bonding, resulting in negligible analyte adsorption. Since both PDMS and glass surfaces are negatively charged under physiological pH conditions, ionic complementary peptides may be ideal coating additives for suppressing EOF and nonspecific analyte adsorption in hybrid PDMS/glass microchannels.

In this study, a facile dynamic coating method using ionic complementary peptide EAK16-II [(Ala-Glu-Ala-Glu-Ala-Lys-Ala-Lys)₂] was developed for the rapid and efficient electrophoretic analysis of carbohydrates in hybrid PDMS/glass microchannels. The separation conditions were systematically investigated with respect to the EAK16-II concentration, running buffer, buffer pH, and electric field strength (E_{sep}). Under the optimal conditions, 8-aminopyrene-1,3,6-trisulfonic acid (APTS)-labeled maltodextrin ladder, glycans from glucosamine capsules, tablets, and pomegranate peel extracts were well separated with high efficiency and reproducibility in the hybrid PDMS/glass microchannels.

2. Experimental

2.1. Chemicals and solutions

Maltodextrin ladder, DDM, and APTS were obtained from Sigma-Aldrich (St. Louis, MO). EAK16-II (>95% pure by HPLC) was synthesized by China Peptides Co., Ltd. (Shanghai, China). Sodium cyanoborohydride (NaBH₃CN), dimethylsulfoxide (DMSO), and all other chemicals were ordered from local commercial suppliers and were of analytical reagent grade unless otherwise specified. Glucosamine capsules and tablets were purchased from a local pharmacy, and glycans PGP from pomegranate peel extracts were prepared as described by Zhou et al. [38]. Deionized (DI) water (Milli-Q, Millipore, Bedford, MA) was used to prepare aqueous solutions. Running buffers containing 1.0 mg/mL EAK16-II were prepared using 10 mM phosphate, 10 mM borate, or 10 mM Tris-HCl buffer containing 0.05% DDM; the solutions were stirred slowly until they appeared homogeneous and transparent. Buffers were adjusted to the desired pH using NaOH.

2.2. Preparation and labeling of samples

Glycans were extracted from glucosamine capsules and tablets and pomegranate peel using solvent grinding extraction, and the final solutions were filtered through 0.22 μm Nylon filters

before labeling. Maltodextrin ladder and extracted glycans were labeled with APTS to impart charges for electrophoresis and render the glycans fluorescent [4,15,23]. Briefly, in a 1.5 mL microcentrifuge tube, 20 μL of 1.0 mg/mL maltodextrin ladder, glucosamine capsule (1.0 g glucosamine hydrochloride/g) and tablet (500 mg glucosamine hydrochloride and 200 mg chondroitin sulfate/g) extracts, or pomegranate peel extracts was mixed with 2 μL of 100 mM APTS in a 0.9 M acetic acid solution and 10 μL of 1.0 M NaBH₃CN in DMSO. The mixture was kept in a water bath at 55 °C for 2.0 h, and then the reaction mixture was diluted with DI water to 100 μL and stored at –20 °C. An aliquot of the above derivatized samples was diluted to the desired concentrations with DI water prior to analysis.

2.3. Fabrication of microchips

The PDMS microfluidic chips were fabricated in PDMS using a rapid prototyping technique, starting with a master composed of a positive relief of negative NR21-20000P resist on a glass slide made using photolithography [31,33,39]. The PDMS base and curing agent were mixed thoroughly at a mass ratio of 10:1, degassed under vacuum, poured onto the master, and cured in a vacuum oven at 70 °C for 90 min. Then, the PDMS replica was peeled from the master, and holes were punched in it (2.5 mm in diameter) to create the reservoirs. Then, it was irreversibly bonded to a 25 mm × 75 mm microscope glass slide using air plasma, forming a hybrid PDMS/glass microchip. The hybrid PDMS/glass microchips had a simple cross channel of 100 μm wide and 30 μm deep.

2.4. Preparation of PDMS and glass surface specimens

PDMS and glass slabs (10 mm × 10 mm) were first sonicated in 1.0 M NaOH and DI water for 30 min and dried under vacuum to obtain PDMS and glass substrates. Then, PDMS and glass sheets were immersed in 10 mM phosphate buffer (pH 6.76) containing 1.0 mg/mL EAK16-II at 25 °C for 1 h. Afterward, PDMS and glass sheets were pulled out of the solution and dried at 25 °C, and then washed thoroughly with DI water and dried under vacuum. Finally, PDMS and glass specimens were characterized by water contact angles (WCAs) measurement, atomic force microscopy (AFM), and X-ray photoelectron spectroscopy (XPS).

2.5. Characterization of PDMS and glass surfaces

WCAs measurements were performed using an OCA 20 optical contact angle meter (Dataphysics, Inc., Stuttgart, Germany) via the sessile drop technique using DI water. The data given were based on ten contact angle measurements at five different positions on the PDMS and glass specimens. The AFM images of the pristine and EAK16-II-coated PDMS and glass surfaces were acquired using a CSPM5500 atomic force microscope (Beijing, China) in tapping mode. The measurements were performed at a scan frequency of 2 Hz using a standard silicon tip with a resonance frequency of 306 kHz. Measurements were made three times at different areas of each PDMS and glass specimen in a scanning area of 2.0 μm × 2.0 μm. XPS analyses were performed using an Axis Ultra X-ray photoelectron spectrometer (Kratos Analytical Ltd., Manchester, UK) with an Al X-ray source operating at 150 W (15 kV, 10 mA). The vacuum in the main chamber was kept above 3 × 10⁻⁹ Pa during XPS data acquisition. The specimens were analyzed at an electron take-off angle of 45° with respect to the surface plane. General survey scans (binding energy range of 0–1200 eV, pass energy of 80 eV) and high-resolution spectra (pass energy of 75 eV) in the C 1s, O 1s, Si 2s, Si 2p, and N 1s regions were recorded

for all modified PDMS and glass substrates. The binding energies (BEs) were referenced to the C 1s binding energy at 284.6 eV.

2.6. Microchip electrophoresis

All μ -CE experiments were carried out on a laboratory-built system based on an inverted fluorescence microscope (Olympus IX51) using a 100 W high-pressure mercury lamp as the excitation radiation source. The light from the mercury lamp was filtered by a 460–490 nm band-pass filter, reflected by a 505 nm dichroic mirror, and then focused on the microchannel by a 20 \times objective (NA 0.45). The emitted fluorescence was collected through the same objective with a 510 nm band-pass filter and captured by a photosensor module (H10722-110, Hamamatsu Photonics, Hamamatsu, Japan). The resulting signals were finally collected and processed with a Model N2000 chromatography workstation (Zhejiang University, Hangzhou, China).

The distances from the channel intersection to the sample (S), sample waste (SW), buffer (B), and buffer waste (BW) wells were 5.25, 5.25, 5.75, and 37.5 mm, respectively. The effective separation channel length was 30 mm. Potentials were applied to the sample, buffer, and waste reservoirs with an HVS448-3000D high-voltage sequencer (from 0 to 1500 V) for the μ -CE experiments. Prior to each experiment, the PDMS microchannels were modified first by flushing them with 100 μ L of a 10 mM running buffer containing EAK16-II and 0.05% DDM. Then, all reservoirs were filled with either the running buffer containing additive or sample using a pipette. For sample loading, 300 V was applied to the SW reservoir while the other three reservoirs were grounded. Following a 30 s sample injection, subsequent separation was triggered by applying a high potential of 1480 V to the waste reservoir and a corresponding potential of 480 V to both the S and SW reservoirs while grounding the buffer reservoir to create the desired field strengths in the separation microchannels.

The EOF in the hybrid PDMS/glass microchannel was measured using previously reported monitoring method [15,33]. Briefly, the reservoirs and the fluidic channels of the hybrid PDMS/glass chip were filled with a 10 mM phosphate buffer, and the contents of the buffer waste reservoir were then replaced with a 5 mM phosphate buffer. The current variation in the fluidic channel was monitored after electrical field being applied to the channel, and the time required for the current to reach a constant level was recorded. The electroosmotic mobility, μ -EOF, was calculated by dividing the channel length by the buffer replacement time and the electric field strength.

2.7. Safety considerations

μ -CE used high voltages; hence, special care should be taken when handling the electrophoresis electrodes to avoid possible electrical shock.

3. Results and discussion

3.1. Separation of APTS-labeled maltodextrin ladder in the hybrid PDMS/glass microchannels dynamically coated with EAK16-II

It is well observed that the concentrations of coating additives significantly influence the dynamic coating and separation performance in μ -CE [4,15,40]. Our previous work showed that DDM can efficiently promote the self-assembly of peptides into a complete and compact coating layer composed predominantly of tightly packed β -sheets on both hydrophobic and hydrophilic PDMS surfaces [33]. Therefore, all running and coating buffers in subsequent experiments contained 0.05% (w/v) DDM. As shown in Fig. 1A, no reproducible separation of APTS-labeled maltodextrin ladder

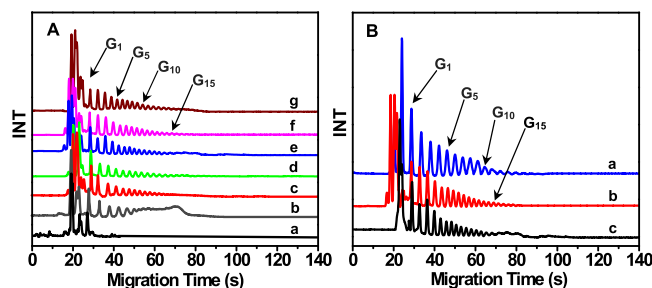


Fig. 1. (A) Microchip electropherograms of APTS-labeled maltodextrin ladder in the hybrid PDMS/glass microchannels dynamically coated with (a) 0.0 (b) 0.1, (c) 0.4, (d) 0.6, (e) 0.8, (f) 1.0, and (g) 1.2 mg/mL EAK16-II-0.05% DDM. Experimental conditions: $E_{\text{sep}} = 270$ V/cm, 10 mM phosphate buffer (pH 6.76). (B) Microchip electropherograms of APTS-labeled maltodextrin ladder in different commonly used buffers in the hybrid PDMS/glass microchannels: (a) 10 mM borate buffer, pH 9.4; (b) 10 mM phosphate buffer, pH 6.76; and (c) 10 mM Tris-HCl buffer, pH 8.0. Experimental conditions: $E_{\text{sep}} = 270$ V/cm, 1.0 mg/mL EAK16-II-0.05% DDM.

was obtained in an uncoated microchannel due to strong analyte adsorption on the microchannel. In contrast, the separations obviously improved with the increased EAK16-II in 10 mM phosphate buffer (pH 6.76), and no further improvement in separation performance was observed at 1.0 mg/mL EAK16-II or above, indicating negligible analyte adsorption in the microchannels. Thus, 1.0 mg/mL EAK16-II containing 0.05% DDM was used in the running buffers. Next, the effect of running buffers on the separation of glycans was investigated including 10 mM phosphate buffer (pH 6.76), 10 mM borate buffer (pH 9.4), and 10 mM Tris-HCl buffer (pH 8.0). As compared with 10 mM Tris-HCl buffer (pH 8.0) and borate buffer (pH 9.4), 10 mM phosphate buffer (pH 6.76) allowed more rapid and reproducible separations of APTS-labeled glycans (Fig. 1B). The baseline separations of more than 15 APTS-labeled glycans in a maltodextrin ladder were achieved with high reproducibility within 70 s at EAK16-II concentrations of 1.0 mg/mL with more than 4.0×10^5 theoretical plates/m. Relative standard deviation (RSD) values less than 3.2% (data obtained in four different microchannels, $n = 4$) were obtained for the migration times of APTS-labeled glycans. Therefore, 10 mM phosphate buffer (pH 6.76) containing 1.0 mg/mL EAK16-II-0.05% DDM was used in the subsequent experiments. Also, the EOF of 10 mM phosphate buffer (pH 6.76) was substantially suppressed from $(+3.45 \pm 0.12) \times 10^{-4} \text{ cm}^2 \text{ V}^{-1} \text{ s}^{-1}$ in an untreated microchannel to $(+0.39 \pm 0.03) \times 10^{-4} \text{ cm}^2 \text{ V}^{-1} \text{ s}^{-1}$ ($n = 4$) in a hybrid PDMS/glass microchannel dynamically coated by 1.0 mg/mL EAK16-II.

3.2. Characterization of EAK16-II coatings on the PDMS and glass surfaces

AFM measurements were conducted to further confirm the existence of EAK16-II self-assembled into a coating layer on both the hydrophobic PDMS and hydrophilic glass surfaces. Fig. 2AI and AIII showed the AFM images of the pristine PDMS and glass surfaces, respectively, which exhibited relatively smooth surfaces with visible ridges and valleys. In contrast, the PDMS and glass surfaces coated with EAK16-II showed discernible ribbon-like structures (arrows in Fig. 2AII and AIV), forming continuous and tight self-assemblies with clearly visible holes. As shown in Table 1, the WCAs of the pristine hydrophobic PDMS and hydrophilic glass substrates were $120.3^\circ \pm 0.4$ and $21.2^\circ \pm 0.3$, respectively, whereas a slightly decreased WCA of $111.4^\circ \pm 0.6$ and a significantly increased WCA of $92.4^\circ \pm 0.7$ were observed for the EAK16-II-coated hydrophobic PDMS and hydrophilic glass surfaces. This indicates that the hydrophobic and hydrophilic sides of EAK16-II were exposed to the solution and the surface, respectively, on both the hydrophobic PDMS and hydrophilic glass surfaces, consistent with previously

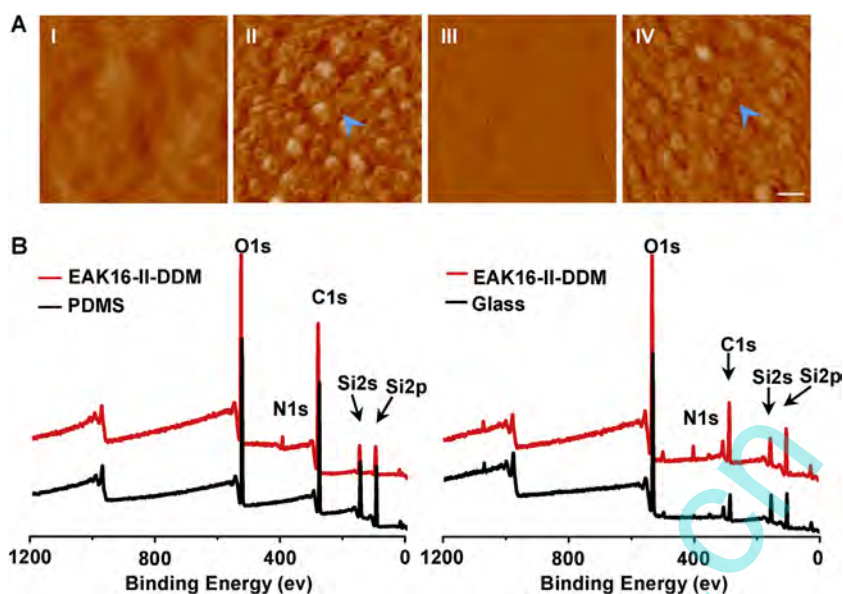


Fig. 2. (A) AFM topography images ($2\ \mu\text{m} \times 2\ \mu\text{m}$) of the pristine PDMS (AI) and glass (AIII), coated PDMS (AII) and glass (AIV) by EAK16-II-0.05% DDM. Scale bar, 500 nm. (B) XPS spectra of the uncoated and EAK16-II-0.05% DDM-coated PDMS and glass surfaces.

Table 1

Water contact angles on the PDMS and glass surfaces coated with EAK16-II-0.05% DDM.

Coating additives	WCA, degrees ^a	
	Hydrophobic PDMS	Hydrophilic Glass
No additives	120.3 ± 0.4	21.2 ± 0.3
1.0 mg/mL EAK16-II-DDM	111.4 ± 0.6	92.4 ± 0.7

^a Data are reported as the mean \pm standard error ($n=6$).

Table 2

Elemental compositions of the uncoated and EAK16-II-0.05% DDM-coated PDMS and glass surfaces determined by XPS.

Substrates	Atomic Concentration (%)					Ratio
	C1s	O1s	Si2p	N1s	O/C	
PDMS	51.45	26.48	22.07	0.00	0.51	
EAK16-II-DDM/PDMS	51.83	38.64	5.66	3.87	0.75	
Glass	23.86	53.26	22.88	0.00	2.23	
EAK16-II-DDM/Glass	38.66	45.73	12.23	3.38	1.18	

reported results [33,36]. The XPS spectra of the pristine PDMS and glass surfaces showed four typical peaks: O1s, C1s, Si2s, and Si2p at 531, 283, 151, and 102 eV, respectively (Fig. 2B). For the EAK16-II-coated hydrophobic PDMS and hydrophilic glass surfaces, N1s peaks appeared at 398 eV, which only belongs to the amine group of a peptide, thus confirming the existence of self-organized peptides on the surfaces. Based on the N 1s content (Table 2), the coverage of EAK16-II on the PDMS and glass surfaces was nearly identical. WCAs and XPS measurements further verified the AFM observations that EAK16-II self-assembled into a complete and compact coating layer tightly adsorbed on both the hydrophobic PDMS and hydrophilic glass surfaces, which greatly suppressed the analyte adsorption and EOF in hybrid PDMS/glass microchannels.

3.3. Optimization of electrophoretic separation conditions

3.3.1. Effect of buffer pH

Because of the three strong negative charges of APTS-labeled maltodextrin ladder, it is very possible to investigate the electrophoretic behavior of APTS-labeled glycans on the hybrid

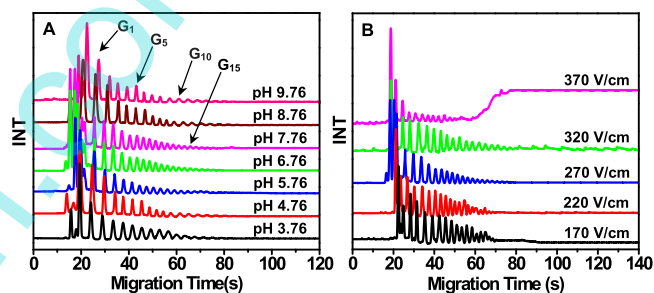


Fig. 3. (A) Effect of buffer pH on separation of APTS-labeled maltodextrin ladder in the hybrid PDMS/glass microchannels. Experimental conditions: $E_{\text{sep}} = 270\ \text{V/cm}$, 1.0 mg/mL EAK16-II-0.05% DDM, 10 mM phosphate buffer at different pH values. (B) Effect of electric field strength on separation of APTS-labeled maltodextrin ladder in the hybrid PDMS/glass microchannels. Experimental conditions: 1.0 mg/mL EAK16-II-0.05% DDM, 10 mM phosphate buffer (pH 6.76).

PDMS/glass microfluidic chips, and if the EAK16-II coating layer on the channel walls is stable, highly reproducible separation under a wide pH range can be achieved. As expected, the separation efficiency of APTS-labeled maltodextrin ladder did not change significantly as buffer pH values increased from 3.76 to 9.76, and remained nearly constant at buffer pH between 6.76 and 7.76, clearly indicating that the EAK16-II coating layer was adsorbed stably on the microchannels and intact after rinsing with copious amounts of buffer. Thus, effective and size-dependent separation was achieved under both acidic and alkaline conditions (Fig. 3A). The baseline separations of more than 15 APTS-labeled glycans were achieved with high efficiency and reproducibility within 80 s with more than 4.5×10^5 theoretical plates/m, and the RSD values were less than 2.4% ($n=4$) for the migration times. Therefore, the buffer pH of 6.76 was selected for the following APTS-labeled glycan separations.

3.3.2. Effect of separation electric field strength

As expected, the field strength in the separation microchannels (E_{sep}) was a key factor in further improvement of the separation efficiencies of APTS-labeled glycans. Owing to the short separation length of microchips, high electric field strength is often desirable for high-performance separation in μ -CE. Therefore, high electric field strength was applied in the hybrid PDMS/glass microchannels

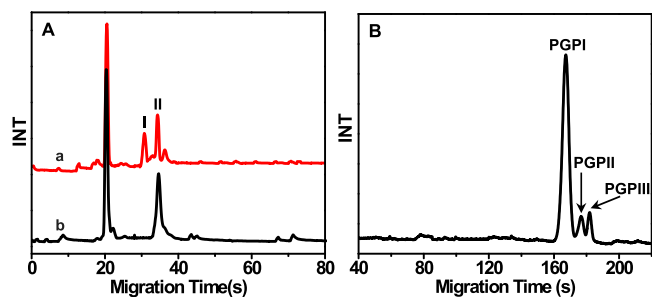


Fig. 4. (A) Microchip electropherograms of carbohydrates extracted from (a) glucosamine tablets and (b) glucosamine capsules: peak I, chondroitin sulfate; peak II, glucosamine hydrochloride. (B) Microchip electropherograms of glycans PGPI, PGPII, and PGPIII from pomegranate peel extracts. Experimental conditions: $E_{sep} = 270$ V/cm, 1.0 mg/mL EAK16-II-0.05% DDM, 10 mM phosphate buffer (pH 6.76).

using an additional high-voltage power supply to achieve reproducible and highly efficient separations. Fig. 3B showed that the separation efficiency increased distinctly with increasing E_{sep} , and then decreased considerably as E_{sep} exceeded 270 V/cm, at which electric current increased irregularly, indicating that Joule heating may lead to peak broadening and should be responsible for the decrease in separation efficiency. The baseline separation of APTS-labeled maltodextrin ladder was achieved in the hybrid PDMS/glass microchannel within 70 s under E_{sep} of 270 V/cm with more than 5.0×10^5 theoretical plates/m, and the RSD values of the migration times were less than 2.0% ($n=4$); therefore, the optimal E_{sep} was approximately 270 V/cm for efficient electrophoretic separation of glycans.

3.4. Sample analysis

The electropherograms showed that the main components were chondroitin sulfate and glucosamine hydrochloride, commercially available dietary supplements similar to calcium preparations, which are widely used for osteoarthritis patients to relieve pain and slow the rate of joint space narrowing and act as first-line pharmacological treatments for long-term control of symptoms of knee osteoarthritis [41,42]. Fig. 4A showed the microchip electropherograms of glycans extracted from glucosamine capsules and tablets. The chondroitin sulfate and glucosamine hydrochloride, which the content is consistent with drug instructions, were well identified in a 30 mm microchannel within 40 s with high efficiency and reproducibility, and these results were in accordance with HPLC results [43].

Pomegranate peel, an important source of polyphenols and other antioxidants, has been used extensively as an ingredient of choice in nutraceuticals and the folk medicine of many cultures owing to its therapeutic properties such as its immunomodulatory, antioxidative, anticancer, and hypoglycemic activity [38,44]. The microchip electropherogram of glycans PGPI, PGPII, and PGPIII from pomegranate peel extracts is shown in Fig. 4B. The baseline separations of PGPI, PGPII, and PGPIII were achieved within 180 s with high reproducibility, which conformed to the previously obtained HPLC results [38]. This approach may provide a quicker and more convenient method to determine the complex carbohydrates in Chinese herbs and Western medicine.

4. Conclusion

In this study, we developed a rapid and reliable electrophoretic separation method for high-performance carbohydrate analyses based on hybrid PDMS/glass microfluidic chips dynamically coated with ionic complementary peptide EAK16-II. This study demonstrated that EAK16-II interacts strongly with the surface negative

charges on both the hydrophobic PDMS and hydrophilic glass surfaces, forming a complete and irreversible coating layer packed tightly on the hybrid PDMS/glass chip surfaces under both acidic and alkaline conditions, which helped to achieve high-performance and reproducible separations of analytes. The proposed method not only provides a universal means for analysis of complex carbohydrates extracted from pharmaceutical or other biological samples, but also opens up new possibilities for the future development of techniques for addressing the nonspecific analyte adsorption and biocompatibility of microfluidic chips fabricated in various materials.

Acknowledgements

This work was supported by the National Natural Science Foundation of China [grant number 21175088].

References

- [1] H.E. Murrey, L.C. Hsieh-Wilson, The chemical neurobiology of carbohydrates, *Chem. Rev.* 108 (2008) 1708–1731.
- [2] S. Mittermayr, J. Bones, A. Guttman, Unraveling the glyco-puzzle: glycan structure identification by capillary electrophoresis, *Anal. Chem.* 85 (2013) 4228–4238.
- [3] M. Delbianco, P. Bharate, S. Varela-Aramburu, P.H. Seeberger, Carbohydrates in supramolecular chemistry, *Chem. Rev.* 116 (2016) 1693–1752.
- [4] F. Dang, K. Kakehi, J. Cheng, O. Tabata, M. Kurokawa, K. Nakajima, M. Ishikawa, Y. Baba, Hybrid dynamic coating with *n*-dodecyl- β -D-maltoside and methyl cellulose for high-performance carbohydrate analysis on poly(methyl methacrylate) chips, *Anal. Chem.* 78 (2006) 1452–1458.
- [5] Q. Fu, T. Liang, X. Zhang, Y. Du, Z. Guo, X. Liang, Carbohydrate separation by hydrophilic interaction liquid chromatography on a 'click' maltose column, *Carbohydr. Res.* 345 (2010) 2690–2697.
- [6] J. Hofmann, H.S. Hahm, P.H. Seeberger, K. Pagel, Identification of carbohydrate anomers using ion mobility-mass spectrometry, *Nature* 526 (2015) 241–244.
- [7] J. Li, M. Chen, Y. Zhu, Separation and determination of carbohydrates in drinks by ion chromatography with a self-regenerating suppressor and an evaporative light-scattering detector, *J. Chromatogr. A* 1155 (2007) 50–56.
- [8] L. Ruhaak, A. Deelder, M. Wuhrer, Oligosaccharide analysis by graphitized carbon liquid chromatography–mass spectrometry, *Anal. Bioanal. Chem.* 394 (2009) 163–174.
- [9] M. Brokl, O. Hernández-Hernández, A.C. Soria, M.L. Sanz, Evaluation of different operation modes of high performance liquid chromatography for the analysis of complex mixtures of neutral oligosaccharides, *J. Chromatogr. A* 1218 (2011) 7697–7703.
- [10] Q. Fu, T. Liang, Z. Li, X. Xu, Y. Ke, Y. Jin, X. Liang, Separation of carbohydrates using hydrophilic interaction liquid chromatography, *Carbohydr. Res.* 379 (2013) 13–17.
- [11] J. Cui, X. Gu, F. Wang, J. Ouyang, J. Wang, Purification and structural characterization of an α -glucosidase inhibitory polysaccharide from apricot (*Armeniaca sibirica* L. Lam.) pulp, *Carbohydr. Polym.* 121 (2015) 309–314.
- [12] S.A. Archer-Hartmann, L.M. Sargent, D.T. Lowry, L.A. Holland, Microscale exoglycosidase processing and lectin capture of glycans with phospholipid assisted capillary electrophoresis separations, *Anal. Chem.* 83 (2011) 2740–2747.
- [13] C. Chen, G.E. Khoury, P. Zhang, P.M. Rudd, C.R. Lowe, A carbohydrate-binding affinity ligand for the specific enrichment of glycoproteins, *J. Chromatogr. A* 1444 (2016) 8–20.
- [14] Q. Zhang, X. Zhang, P. Wang, D. Li, G. Chen, P. Gao, L. Wang, Determination of the action modes of cellulases from hydrolytic profiles over a time course using fluorescence-assisted carbohydrate electrophoresis, *Electrophoresis* 36 (2015) 910–917.
- [15] F. Dang, L. Zhang, H. Hagiwara, Y. Mishina, Y. Baba, Ultrafast analysis of oligosaccharides on microchip with light-emitting diode confocal fluorescence detection, *Electrophoresis* 24 (2003) 714–721.
- [16] E.R. Castro, A. Manz, Present state of microchip electrophoresis: state of the art and routine applications, *J. Chromatogr. A* 1382 (2015) 66–85.
- [17] M. Garcia, A. Escarpa, Microchip electrophoresis–copper nanowires for fast and reliable determination of monosaccharides in honey samples, *Electrophoresis* 35 (2014) 424–425.
- [18] M. Becker, T. Zweckmair, A. Forneck, T. Rosenau, A. Potthast, F. Liebner, Evaluation of different derivatisation approaches for gas chromatographic–mass spectrometric analysis of carbohydrates in complex matrices of biological and synthetic origin, *J. Chromatogr. A* 1281 (2013) 115–126.
- [19] J.D. Oliver, M. Gaborieau, E.F. Hilder, P. Castignolles, Simple and robust determination of monosaccharides in plant fibers in complex mixtures by capillary electrophoresis and high performance liquid chromatography, *J. Chromatogr. A* 1291 (2013) 179–186.

- [20] B. Rühmann, J. Schmid, V. Sieber, Fast carbohydrate analysis via liquid chromatography coupled with ultra violet and electrospray ionization ion trap detection in 96-well format, *J. Chromatogr. A* 1350 (2014) 44–50.
- [21] S. Rodríguez-Sánchez, M.J. García-Sarrió, J.E. Quintanilla-López, A.C. Soria, M.L. Sanz, Analysis of iminosugars and other low molecular weight carbohydrates in *Aglaonema* sp. extracts by hydrophilic interaction liquid chromatography coupled to mass spectrometry, *J. Chromatogr. A* 1423 (2015) 104–110.
- [22] L.M. de Souza, N. Dartora, C.T. Scoparo, P.A. Gorin, M. Iacomini, G.L. Sasaki, Differentiation of flavonol glucoside and galactoside isomers combining chemical isopropylidenation with liquid chromatography-mass spectrometry analysis, *J. Chromatogr. A* 1447 (2016) 64–71.
- [23] F. Dang, E. Maeda, T. Osafune, K. Nakajima, K. Kakehi, M. Ishikawa, Y. Baba, Carbohydrate protein interactions investigated on plastic chips statically coated with hydrophobically modified hydroxyethylcellulose, *Anal. Chem.* 81 (2009) 10055–10060.
- [24] A.C. Siegel, S.K. Tang, C.T. Nijhuis, M. Hashimoto, S. Phillips, M.D. Dickey, G.M. Whitesides, Cofabrication: a strategy for building multicomponent microsystems, *Acc. Chem. Res.* 43 (2010) 518–528.
- [25] P. Neuzil, S. Giselbrecht, K. Länge, T.J. Huang, A. Manz, Revisiting lab-on-a-chip technology for drug discovery, *Nat. Rev. Drug Discov.* 11 (2012) 620–632.
- [26] J. Esquivel, J. Colomer-Farrarons, M. Castellarnau, M. Salleras, F. Campo, J. Samitier, P. Miribel-Català, N. Sabaté, Fuel cell-powered microfluidic platform for lab-on-a-chip applications: integration into an autonomous amperometric sensing device, *Lab Chip* 12 (2012) 4232–4235.
- [27] K. Ren, J. Zhou, H. Wu, Materials for microfluidic chip fabrication, *Acc. Chem. Res.* 46 (2013) 2396–2406.
- [28] P.N. Nge, C.I. Rogers, A.T. Woolley, Advances in microfluidic materials functions, integration and applications, *Chem. Rev.* 113 (2013) 2550–2583.
- [29] C.T. Culbertson, T.G. Mickleburgh, S.A. Stewart-James, K.A. Sellens, M. Pressnall, Micro total analysis systems: fundamental advances and biological applications, *Anal. Chem.* 86 (2014) 95–118.
- [30] N.T. Tran, I. Ayed, A. Pallandre, M. Taverna, Recent innovations in protein separation on microchips by electrophoretic methods: an update, *Electrophoresis* 31 (2010) 147–173.
- [31] L. Yang, L. Li, Q. Tu, L. Ren, Y. Zhang, X. Wang, Z. Zhang, W. Liu, L. Xin, J. Wang, Photocatalyzed surface modification of poly(dimethylsiloxane) with polysaccharides and assay of their protein adsorption and cytocompatibility, *Anal. Chem.* 82 (2010) 6430–6439.
- [32] J. Zhou, D.A. Khodakov, A.V. Ellis, N.H. Voelcker, Surface modification for PDMS-based microfluidic devices, *Electrophoresis* 33 (2012) 89–104.
- [33] X. Yu, J. Xiao, F. Dang, Surface modification of poly(dimethylsiloxane) using ionic complementary peptides to minimize nonspecific protein adsorption, *Langmuir* 31 (2015) 5891–5898.
- [34] H. Jeon, Y. Kim, G. Lim, Continuous particle separation using pressure-driven flow-induced miniaturizing free-flow electrophoresis (PDF-induced μ -FFE), *Sci. Rep.* 6 (2016) 19911–19919.
- [35] M. Tonin, N. Deschames, R. Houdré, Hybrid PDMS/glass microfluidics for high resolution imaging and application to subwavelength particle trapping, *Lab Chip* 16 (2016) 465–470.
- [36] N. Li, J. Xiao, X. Hai, K. Wang, F. Dang, Key role of ionic hydrogen bonding in nonspecific protein adsorption on a hydrophobic surface, *J. Phys. Chem. C* (2016), <http://dx.doi.org/10.1021/acs.jpcc.6b05176>.
- [37] X. Peng, L. Zhao, G. Du, X. Wei, J. Guo, X. Wang, G. Guo, Q. Pu, Charge tunable zwitterionic polyampholyte layers formed in cyclic olefin copolymer microchannels through photochemical graft polymerization, *ACS Appl. Mater. Interfaces* 5 (2013) 1017–1023.
- [38] X. Zhou, J. Zhang, R. Xu, X. Ma, Z. Zhang, Aqueous biphasic system based on low-molecular-weight polyethylene glycol for one-step separation of crude polysaccharides from *Pericarpium granati* using high-speed countercurrent chromatography, *J. Chromatogr. A* 1362 (2014) 129–134.
- [39] Y. Li, C. Liu, X. Feng, Y. Xu, B. Liu, Ultrafast microfluidic mixer for tracking the early folding kinetics of human telomere G-quadruplex, *Anal. Chem.* 86 (2014) 4333–4339.
- [40] A.M. Al-Hossaini, L. Suntornsuk, S.M. Lunte, Separation of dynorphin peptides by capillary electrochromatography using a polydiallyldimethylammonium chloride gold nanoparticle-modified capillary, *Electrophoresis* 00 (2016) 1–8.
- [41] D. Clegg, D. Reda, C. Harris, M. Klein, J. O'Dell, M. Hooper, J. Bradley, C. Bingham III, M. Weisman, Glucosamine chondroitin sulfate, and the two in combination for painful knee osteoarthritis, *New Engl. J. Med.* 354 (2006) 795–808.
- [42] H. Luo, W. Li, D. Ji, G. Zuo, G. Xiong, Y. Zhu, L. Li, M. Han, C. Wu, Y. Wan, One-step exfoliation and surface modification of lamellar hydroxyapatite by intercalation of glucosamine, *Mater. Chem. Phys.* 173 (2016) 262–267.
- [43] Z. Niu, L. Yuan, X. Ye, Z. Sun, J. Wang, L. Ji, Simultaneous HPLC determination of chondroitin sulfate and glucosamine hydrochloride, *Chin. J. Pharm. Anal.* 26 (2006) 802–804.
- [44] C. Zhu, X. Zhai, L. Li, X. Wu, B. Li, Response surface optimization of ultrasound-assisted polysaccharides extraction from pomegranate peel, *Food Chem.* 177 (2015) 139–146.